# The quassinoid derivative NBT-272 targets both the AKT and ERK signaling pathways in embryonal tumors

Castelletti, D ; Fiaschetti, G ; Di Dato, V ; Ziegler, U ; Kumps, C ; De Preter, K ; Zollo, M ; Speleman, F ; Shalaby, T ; De Martino, D ; Berg, T ; Eggert, A ; Arcaro, A ; Grotzer, M A

Abstract: The quassinoid analogue NBT-272 has been reported to inhibit MYC, thus warranting a further effort to better understand its preclinical properties in models of embryonal tumors (ET), a family of childhood malignancies sharing relevant biological and genetic features such as deregulated expression of MYC oncogenes. In our study, NBT-272 displayed a strong anti-proliferative activity in vitro that resulted from the combination of diverse biological effects, ranging from G1/S arrest of the cell cycle to apoptosis and autophagy. The compound prevented the full activation of both the eukaryotic initiation factor 4E (eIF4E) and its binding protein 4EBP-1, regulating cap-dependent protein translation. Interestingly, all responses induced by NBT-272 in ET could be attributed to interference with two main pro-proliferative signaling pathways, i.e. the AKT and the MEK/extracellular signal-regulated kinase (ERK) pathways. These findings also suggested that the depleting effect of NBT-272 on MYC protein expression occurred via indirect mechanisms, rather than selective inhibition. Finally, the ability of NBT-272 to arrest tumor growth in a xenograft model of neuroblastoma plays a role in the strong anti-tumor activity of this compound, both in vitro and in vivo, with its potential to target cell-survival pathways that are relevant for the development and progression of ET.

DOI: https://doi.org/10.1158/1535-7163.MCT-10-0539

Molecular Cancer Therapeutics

# The quassinoid derivative NBT-272 targets both the AKT and ERK signaling pathways in embryonal tumors

Deborah Castelletti, Giulio Fiaschetti, Valeria Di Dato, et al.

*Mol Cancer Ther* Published OnlineFirst October 1, 2010.

# The quassinoid derivative NBT-272 targets both the AKT and ERK signaling pathways in embryonal tumors

Deborah Castelletti[1], Giulio Fiaschetti[1], Valeria Di Dato[2], Urs Ziegler[3], Candy Kumps[4], Katleen De Preter[4], Massimo Zollo[2], Frank Speleman[4], Tarek Shalaby[1], Daniela De Martino[2], Thorsten Berg[5], Angelika Eggert[6], Alexandre Arcaro[7], and Michael A. Grotzer[1]

[1]Dept. Oncology, University Children's Hospital of Zurich, Switzerland; [2]Dept. Biochemistry and Medical Biotechnology, University of Naples, Italy; [3]Center for Microscopy and Image Analysis University of Zurich, Switzerland; [4]Center for Medical Genetics Ghent, Belgium; [5]Inst. for Organic Chemistry, University of Leipzig, Germany; [6]Dept. Oncology, University Children's Hospital of Essen, Germany, [7]Div. Pediatric Hematology/Oncology, Dept. Clinical Research, University of Bern, Switzerland.

**Running title:** Effect of the quassinoid NBT-272 in embryonal tumors

**Key words:** embryonal tumors, ERK, AKT, MYC, protein synthesis

**Abbreviations:** ET, embryonal tumors; MB, medulloblastoma; NB, neuroblastoma; aCGH, array comparative genomic hybridization; IHC, immunohistochemistry; PI, propidium iodide; TEM, transmission electron microscopy; eIF4E, eukaryotic initiation factor 4E; 4EBP-1, 4E binding protein; MAPK, mitogen-activated protein kinase; ERK, MEK/extracellular signal-regulated kinase; mTOR, AKT/mammalian target of rapamycin; S6K, S6 kinase; PI3K, phosphoinositide-3 kinase; CCN, cyclin; CDK, cyclin dependent kinase; RB, retinoblastoma; SQSTM1, sequestosome.

**Notes:**

**Financial support:** Deborah Castelletti and Giulio Fiaschetti were supported by the European Community FP6, project STREP (EET-pipeline, number: 037260). Valeria Di Dato and Daniela De Martino were supported by FP6-EET pipeline LSH-CT-2006-037260 (MZ), FP7-Tumic HEALTH-F2-2008-201662 (MZ), Associazione italiana contro la lotta al Neuroblastoma "Progetto Pensiero" (MZ), and AIRC Tumori Pediatrici 2007- 2010 (MZ).

**Reprint requests to**: Michael A. Grotzer, Steinwiesstrasse 75, University Children's Hospital of Zurich, 8032 Zurich, Switzerland. Telephone: +41 44 266 71 11; Fax: +41 44 2667171; Email: Michael.Grotzer@kispi.uzh.ch

**Disclosure of potential conflicts of interest:** No potential conflicts of interest.

## Abstract

The quassinoid analogue NBT-272 has been reported to inhibit MYC, thus warranting a further effort to better understand its preclinical properties in models of embryonal tumors (ET), a family of childhood malignancies sharing relevant biological and genetic features such as deregulated expression of MYC oncogenes.

In our study, NBT-272 displayed a strong anti-proliferative activity *in vitro* that resulted from the combination of diverse biological effects, ranging from G1/S arrest of the cell cycle to apoptosis and autophagy. The compound prevented the full activation of both the eukaryotic initiation factor 4E (eIF4E) and its binding protein 4EBP-1, regulating cap-dependent protein translation. Interestingly, all responses induced by NBT-272 in ET could be attributed to interference with two main pro-proliferative signaling pathways, i.e. the AKT and the MEK/extracellular signal-regulated kinase (ERK) pathways. These findings also suggested that the depleting effect of NBT-272 on MYC protein expression occurred via indirect mechanisms, rather than selective inhibition. Finally, the ability of NBT-272 to arrest tumor growth in a xenograft model of neuroblastoma plays a role in the strong anti-tumor activity of this compound, both *in vitro* and *in vivo*, with its potential to target cell-survival pathways that are relevant for the development and progression of ET.

## Introduction

Embryonal tumors (ET) represent an important group of childhood malignancies arising from different tissues of fetal origin (1, 2). Medulloblastoma (MB) is a tumor of the central nervous system, originating from granular progenitor cells of the cerebellum (3) and accounting for about 20% of all childhood brain tumors (4). Neuroblastoma (NB) is the most common extra-cranial solid cancer in children originating from the sympathetic nervous system (5, 6). Constant progress has been achieved in clinical practice by increasing the overall survival rate of MB and NB patients although novel therapeutic strategies are still needed, particularly to treat the high-risk patients characterized by a more aggressive disease and poor prognosis. In both MB and NB, high grade malignancy is often associated with overexpression or amplification of MYC oncogenes (7-11) playing a role in embryogenesis and, if aberrantly expressed, in tumor development as well (12).

There is a long history of therapeutic benefits produced by natural compounds and some of these have formed the backbone for further targeted chemical modifications improving efficacy and selectivity. Quassinoids have been investigated for their anti-neoplastic properties (13), which has led to the identification of interesting candidates such as bruceantin, with significant inhibitory effects on leukemia, lymphoma, and myeloma cell growth, both *in vitro* and *in vivo* (14). Bruceantin was reported to induce apoptosis and cell differentiation, thus justifying efforts to develop quassinoid analogues with improved efficacy.

Among the derivatives of bruceantin, NBT-272 displayed a significantly stronger toxicity compared to the parent molecule, as tested in different models of hematological and solid tumors (15, 16). Moreover, NBT-272 was reported to induce downregulation of c-MYC in

MB-derived cells (16), thus raising the question of the mechanisms underlying NBT-272's cytotoxicity and its selectivity for MYC in ET.

Besides activating programmed cell death, quassinoids were shown to arrest cell growth by impairing protein synthesis mediated by the eukaryotic translation initiation factor 4E (eIF4E) (17). The phosphorylation status of eIF4E plays an important biological role in modulation of normal cell growth in response to extracellular stimuli and during development (18). However, eIF4E was also reported to be an oncogene (19) and its transformation properties were attributed, at least in part, to induction of cell cycle progression through cyclin D1 and MYC (20). Activation of eIF4E itself is mainly regulated by two pathways, namely the mitogen-activated protein kinase (MAPK) pathway (21) and the AKT/mammalian target of rapamycin (mTOR) pathway via the 4E binding protein (4EBP-1) (22).

In the present study, we have investigated the effect of NBT-272 in different cellular models of ET, both *in vitro* and *in vivo*. The compound triggered multiple cellular responses, ranging from cell cycle arrest to induction of autophagy, which are downstream effector mechanisms of the AKT/mTOR and ERK pathways. In turn, interference with these signaling events could also explain the inhibitory effect of NBT-272 on protein synthesis and on expression of c-MYC/MYCN in different ET entities.

## Materials and Methods

### Cell lines

The following human cell lines were used: the neuroblastoma SK-N-BE, SH-SY5Y, and WAC-2 (23) (G. M. Brodeur, Children's Hospital, Philadelphia, MA), retinoblastoma Y79 and WERI (A. Eggert, University Children's Hospital, Essen, Germany), Ewing's sarcoma family of tumors (ESFT) A673 and TC71 (H. Kovar, St. Anna Children's Cancer Research Institute, Vienna, Austria), malignant rhabdoid tumor (MRT) LP and MON (O. Delattre, Institut Curie, Paris, France). Medulloblastoma DAOY and D341 were purchased from American Type Culture Collection (ATCC). Cells that were not purchased from ATCC were authenticated by comparative genomic hybridization (in the laboratories mentioned above or as described below). The clone DAOY M2 (overexpressing c-MYC) was kindly provided by D. Stearns (Johns Hopkins University, Baltimore, MD) (11). NB, ESFT, and MRT cell lines were grown in RPMI medium (Life Technologies/Invitrogen, Carlsbad, CA) supplemented with 10% (v/v) fetal calf serum (FCS) and penicillin/streptomycin (PS)/L-glutamine, whereas RB cells were grown in DMEM (Invitrogen, Carlsbad, CA) supplemented with 15% (v/v) FCS Gold (Invitrogen ), 10 μg/ml insulin (Sigma-Aldrich, St. Louis, MO), 50 μM 2-β-mercaptoethanol (Sigma-Aldrich), and PS/L-glutamine. MB cells were cultured in Richter's zinc option medium (Invitrogen) supplemented with 10% (v/v) FCS and PS/L-glutamine.

### Array CGH

The ET-derived cell lines used in the study were profiled by array comparative genomic hybridization (aCGH) using a custom 60K Embryonal Tumor array CGH-chip (ET-aCGH chip) (Agilent Technologies, Santa Clara CA), as described by Kumps et al. (BMC Genomics, in press).

**Cell viability, clonogenic, and apoptosis assays**

The 3-(4,5-dimethylthiazol-2-yl)-5-(3-carboxymethoxyphenyl)-2-(4-sulfophenyl)-2H-tetrazolium (MTS)-based CellTiter 96® AQueous One assay (Promega, Madison, WI) was used to quantify cell viability. Colony formation in agar was tested by seeding single cells (4,000 per well) in agar-containing medium (0.35% (w/v) final concentration) on top of a 0.5% (w/v) agar-layer. Apoptosis was investigated by quantifying the activation of caspases, by using the Caspase-Glo 3/7 Assay (Promega) according to the manufacturer's instructions. The *In Situ* Cell Death Detection Kit (Roche, Mannheim, Germany) was also employed to evaluate the pro-apoptotic response of ET cells. The TUNEL reaction was performed in the presence of fluorescein-labeled nucleotides and followed by detection under a fluorescent microscope (Axioskop 2, Zeiss).

**Cell cycle analysis**

Cells (5-10x$10^5$) were treated for the indicated time-intervals with different doses of NBT-272 or mock-treated (control). After washing with PBS, cells were washed and harvested in a 2 mM EDTA/PBS solution. Cell pellets were fixed with ice-cold 70% ethanol on ice for 40-60 min and, after centrifugation at 2500 g for 5 min, resuspended with 50 µg/ml propidium iodide (PI)/PBS containing 100 U/ml RNAase (Sigma-Aldrich). The DNA content was estimated by using a BD FACS Canto II flow cytometry system for acquisition and the Flojo software for the data analysis.

**Gene expression analysis by PCR arrays**

Total RNA from DAOY, D341, SK-N-BE, and SH-SY-5Y cells, treated with 20 nM NBT-272 for 24 h or left untreated, was subjected to reverse transcriptase (RT) (RT² First Strand Kit, SABiosciences, Frederick, MD). The resulting cDNA was used as a template for RT²

Profiler™ PCR Array (SABiosciences) for pathway-focused gene expression analysis (using sets of arrayed TaqMan probes for cell cycle and apoptosis genes). Gene expression was expressed as log2Ratio (Ratio=2^-ΔΔCt), relative to normalization to untreated control samples and to the average expression of 5 house-keeping genes (B2M, HPRT1, RPL13A, GAPDH, and ACTB). Only statistically significant gene expression changes over three independent experiments were considered.

**Western blot analysis**

Total cell lysates were prepared in RIPA buffer (50 mM Tris-HCl, pH 7.5, 0.1% sodium laurilsulfate, 0.1% sodium deoxycholate, 150 mM NaCl, 1% NP40, 1 mM EDTA, and 1 mM EGTA), supplemented with protease inhibitors (Roche) and phosphatase inhibitors (10 mM sodium fluoride, 10 mM sodium orthovanadate, and 10 mM sodium β-glycerophosphate. The amount of protein was determined by BCA Protein Assay (Pierce, Rockford, IL). Cell lysates in SDS-sample buffer were boiled for 8 min and equal protein amounts were resolved by 4-12% gradient SDS-PAGE and immunoblotting using PVDF membranes. The antibodies reacting against the following proteins were employed: cyclin D1, caspase-3, AKT, mTOR, phospho-ERK 1/2(Tyr202/204) (Santa Cruz Biotechnology, Santa Cruz, CA); ERK, phospho-AKT(Ser473), phospho-MEK1/2(Ser217/221), phospho-RB(Ser795), RB, phospho-S6 (Ser235/236), S6, phospho-mTOR(Ser2248), phospho-MNK1(Thr197/202), MNK1, phospho-eIF4E(Ser209), eIF4E, 4EBP-1, phospho-4EBP-1(Thr37/46), cyclin E, CDK2, CDK4, PARP, LC-3, c-MYC, MYCN, and ATG5 (Cell Signaling, Danvers, MA); β-tubulin and β-actin antibodies were from Sigma-Aldrich, whereas the anti-SQSTM1/p62 was purchased from BIOMOL International. In order to inhibit proteasome-dependent protein degradation, cells were treated with 50 μM MG-132 (Sigma-Aldrich). The PI3K/mTOR inhibitor BEZ-235 was purchased by Axon Medchem.

**Transmission Electron Microscopy**

After treatment (with NBT-272, rapamycin, or vehicle) for different time-intervals, DAOY and SK-N-BE cells were subjected to fixation at room temperature for 30 min with 2% glutaraldehyde and 0.8% formaldehyde in 50 mM sodium cacodylate (pH 7.3), followed by 30 min exposure to 1% $OsO_4$ and 1.5% $K_4Fe(CN)_6$ in 50 mM sodium cacodylate (pH 7.3). Fixed samples were contrasted using 2% uranyl acetate in water for 2 h, progressively dehydrated in increasing concentrations of ethanol, and embedded into epon (Catalys, Duebendorf, Switzerland). Ultrathin sections of 50 nm were prepared and contrasted with uranyl acetate and lead citrate. Samples were analyzed by using a CM 100 transmission electron microscope (Philips, Leiden, Netherlands).

***In vivo* xenograft model**

Human NB SH-SY5Y cells were stably transfected with a pLentiV5-Luciferase-expressing vector (Invitrogen) as described elsewhere (24). SH-SY5Y-LUC clones were grown under standard conditions in Dulbecco's Modified Eagle's Medium (DMEM) containing 10% (v/v) FCS, L-glutamine, and blasticidine for selection.

Eight-weeks-old female athymic nude mice from Harlan Laboratories (Udine, Italy) were inoculated subcutaneously in the right rear flank with $2x10^6$ SHSY5Y-LUC cells, injected in 100 µl PBS solution. Tumor cell growth was monitored weekly by measuring luminescence emission, referred to as bioluminescence imaging (BLI) levels, using the IVIS 3D Illumina Imaging System (Xenogen Corp. Alameda, CA). A detailed procedure is available by Caliper. The BLI/tumor size ratio was quantified by encircling the luciferase-emitting areas using the Living Images Software 3.2 (Xenogen, Alameda, CA). Three weeks after implantation, the mice were divided into two homogeneous groups based on their BLI level (photon/sec/cm²).

Each group received either 10 µM/week of NBT-272 or vehicle (EtOH 0.003%/PBS), administered as 100 µl solution each time, three times a week. The analysis of the tumor growth was performed 3, 4, and 6 weeks after the first NBT-272 administration. The dose was adjusted by taking into account preliminary data provided by NaPro Bio Therapeutics, Inc. (MTD=0.9 mg/Kg/week) (15) and the *in vitro* results. The treatment was performed for 6 weeks before the animals were sacrificed and tumor samples were analysed by immunohistochemistry and western blotting. Quantitative data analysis of the tumor size was performed by ANOVA statistical tests, using the Statview program.

All animal experiments were conducted according to national and international guidelines and following approval by the Institutional Animal Care and Ethical Committee of CEINGE-University of Naples Federico II (Protocol #29 - 30/09/2009) and of the Italian Ministry of Health (Dipartimento Sanità Pubblica Veterinaria D.L. 116/92).

**Immunohistochemistry**

Paraffin embedded tumor samples were treated with xylene, heated for 45 min (in citrate buffer, pH 6.0), and finally treated 15 min with 1% $H_2O_2$ (Carlo Erba Reagents, Rodano, Italy). Tissues for immunohistochemistry (IHC) were blocked with 3% BSA-5% total goat serum-0.3% Tween 20/PBS (1 h, room temperature). Primary antibodies reactive against human Ki67 (M7240, Dako) and human cleaved caspase-3 (9661, Cell Signaling) were used (1 h, room temperature, diluted 1:100 in blocking solution). After incubation with a biotin-conjugated secondary antibody (1 h, room temperature), the detection was performed in the presence of 3,3'-diaminobenzidin (Dako, Glostrup, Denmark) according to the manufacturers' protocol. The sections were counterstained by hematoxylin/eosin (H&E) (Bio Optica, Milano, Italy), washing three times with 0.2% Triton X-100/PBS after every incubation steps. As negative control, blocking solution was used instead of the primary antibody.

## Results

**NBT-272 strongly impaired cell growth in ET-derived cell lines.** NBT-272 (NaPro Bio Therapeutics, Inc.) (Fig. 1A) is a semi-synthetic analogue of bruceantin (14, 17), with 10-fold higher toxicity than the parent compound *in vitro* (15). Previously published data showed the ability of NBT-272 to drastically reduce the protein expression level of the oncogene c-MYC in MB-derived cell lines (16), although the exact mechanism of action remained unexplored. In the present study, the biological responses induced by NBT-272 were investigated in a panel of 13 cell lines, representative of six different ET entities (Fig. 1). Expression of c-MYC and MYCN was evaluated in each cell line both at protein (Fig. 1SA) and mRNA levels (Fig. 1SB); these varied significantly, reflecting the gene expression ranging from single copy to gene amplification.

The ET cell lines were profiled for copy number changes (gain/loss) using aCGH. In Fig. 2S, the aCGH data of 8 cell lines are reported. Some cell lines displayed very few genomic aberrations (1q gain in the MRT cells LP, and 1q gain and 8 gain in MB D341), whereas others have very complex profiles, such as WERI cells with a 1q-gain region that appeared very discontinuous.

The effect of NBT-272 was first evaluated in terms of cell viability, clearly showing a very potent effect of the compound in all selected ET-derived cell lines (Fig. 1B, C). The $IC_{50}$ values, calculated from the dose-response curves, varied in the nM range of concentration, i.e. about two orders of magnitude lower compared to many small-molecule inhibitors investigated as anti-cancer drugs. Additionally, five representative ET cell lines (WAC-2, SK-N-BE, A673, MON, Wit-49) were tested for anchorage-independent growth in soft agar in the presence of NBT-272 (Fig. 1D). The compound reduced colony formation by 50% (compared

with mock-treated controls) at doses that were similar or lower than the $IC_{50}$ obtained in cell viability assays (Fig. 1C).

**NBT-272 induced cell cycle arrest at the G1/S transition.** In order to identify which molecular characteristics were responsible for NBT-272's toxicity, we sought to investigate the diverse biological responses triggered in ET cell lines by the compound. The effect on cellular distribution at different stages of the cell cycle was evaluated by DNA staining in MB and NB cells. In dose-response experiments at different time points, 5 nM NBT-272 was already sufficient to almost halve the population of replicating DAOY cells after 24 h, with a concomitant increase in G1 population (Fig. 3S). This observation was found to extend to NB cell lines (WAC-2, SK-N-BE, and SH-SY5Y) (Fig. 2A). Here, NBT-272 induced a similar effect after 16 h treatment, thus suggesting that blocking the cell cycle progression at the G1 to S transition occurs as one of the earliest mechanisms leading to proliferative arrest.

Consistent with the data obtained by cytofluorimetry, NBT-272 induced loss of cyclin D1 (CCND1) and of its interacting partner the cyclin dependent kinase (CDK)4 (Fig. 2B). These proteins are both important regulators of the cell cycle progression through the G1 phase (25), along with the phosphorylation status of RB, which changes throughout the cell cycle with highest levels when cells enter the S phase (26). Consistent with an arrest in the G1/S transition, RB was hypophosphorylated on treatment with NBT-272 (Fig. 2B). On the contrary, the effect on CCNE1/CDK2 was transient.

Two NB cell lines (SH-SY5Y and SK-N-BE) and the MB cells DAOY and D341 were treated for 24 h with 20 nM NBT-272, followed by expression profiling of 84 cell cycle-related genes by qRT-PCR. Fig. 4SA illustrates the statistically significant gene expression changes induced by NBT-272. The 23 transcripts fell into three functional categories: i) G1/S transition of the cell cycle; ii) DNA damage (e.g. growth arrest and DNA damage-inducible

alpha protein, GADD45A); and iii) regulation of transcription elongation. The most relevant changes concerned genes involved in the G1 arrest, in support of the data from our biological assays (Fig. 2). For instance, consistent with a G1/S block of the cell cycle, the mRNA level of CDK2 decreased, while the inhibitor molecules CDKN1A/p21$^{Cip1}$and CDKN1B/p27$^{Kip}$ were induced on treatment (Fig. 4SA). Whereas CCND1 and CCNE1 were regulated solely at the protein level (Fig. 2B), other cyclins and CDK molecules involved in the RNA polymerase II-mediated gene transcription (CCNC/CDK8, CCNH/CDK7, and CCNT/CDK9) were found to be upregulated.

**Apoptosis was induced by NBT-272 in a cell type-dependent manner.** Induction of apoptosis was assessed by quantifying activation of caspases-3/7 induced by NBT-272 (Fig. 3A). The pro-apoptotic response to NBT-272 varied significantly in a cell type- and tumor-dependent way. This observation was also confirmed by Cell Death ELISA assays (Roche) (not shown). Whereas NBT-272 concentrations as small as 10 nM triggered apoptosis in MB-, ESFT-, and MRT-derived cell lines after 24 h, the same doses had a very modest pro-apoptotic effect in other cellular models, particularly in NB (Fig. 3A). The limited pro-apoptotic effect of NBT-272 in MB and NB cells was also shown by immunoblotting (Fig. 3B), where caspase-3 could be only detected as full length protein and PARP cleavage was only induced in MB cell lines (e.g. in D341, Fig. 3B). This observation was confirmed by TUNEL assay, where NBT-272 was able to induce a breakage of the genomic DNA in DAOY cells (Fig. 5S).

Using a similar approach to that employed for cell cycle-related genes, we investigated the transcriptional changes related to apoptosis triggered by NBT-272 (Fig. 4SB). Among the differentially expressed genes, we found key components of both the extrinsic and the intrinsic pathways of apoptosis, mainly upregulated on treatment with the compound. This

was the case with pro-apoptotic members of the Bcl-2 family (BIK, BAD, and BAK) and with proteins bearing the caspase recruitment domain (CARD), such as Bcl-10, PYCARD and RIPK2, implicated in the recruitment and binding of caspases. Another major group, namely genes encoding for ligands and receptors of the tumor necrosis factor (TNF) superfamily, was induced (Fig. 4SB). It included TNF-α, TNF-β/LTA, TNFSF10/TRAIL and their corresponding receptors TNFRSF10A and TNFRSF10B. Also the expression of TNFRSF5, TNFRSF9, and TNFRSF6/FAS increased on NBT-272 treatment, altogether indicating enhanced cell responsiveness to death receptors-mediated signaling.

**NBT-272 triggered autophagosome formation.** Because NBT-272 induced apoptosis with differing efficiency in the ET cell lines tested, we sought additional mechanisms that could lead to cell death. Formation of the distinctive traits of autophagy was investigated at the ultrastructure-cellular level by transmission electron microscopy (TEM), thus revealing induction of a high number of double-membrane structures containing cellular material (i.e. cytosolic cargo molecules and organelles), described as autophagosomes (27).

In Fig. 3C, TEM images of DAOY (MB) and SK-N-BE (NB) cells are reproduced. Compared with mock-treated controls (panels a, b), treated cells (20 nM NBT-272, 16 h) displayed all the characteristic signs of autophagy induction, in particular formation of large autophagosomes (arrow heads in panels e, f, g) and increased lysosomes and vacuoles. Moreover, the cytosol appeared looser than in control cells, the nuclear envelope became irregular, the mitochondria acquired swollen crests indicative of dysfunctional activity, and myelin figures could be visualized as electron-dense structures. As positive control, DAOY cells were treated separately with rapamycin (200 nM, 48 h) (panel h), inducing autophagy as an event associated with inhibition of mTOR (28). On comparing the effect of the two compounds in DAOY cells, NBT-272 proved to be a much stronger inducer of autophagy.

Formation of autophagosomes requires a rather complex rearrangement of Atg proteins, including the protein conjugation system generating the complex Atg5-Atg12 (29), which was detected by immunoblotting, on treatment of DAOY cells with 20 nM NBT-272 (Fig. 3D). Concomitantly, we were able to demonstrate the degradation of sequestosome 1 (SQSTM1/p62), i.e. a multifunctional adaptor molecule driving the degradation of polyubiquitinated proteins such as those tagged for autophagic clearance (30). Further, we documented the conversion of the microtubule-associated protein light chain 3 (LC3-I) into its membrane-interacting counterpart (LC3-II), which is a well documented marker of autophagy induction.

**MYC depletion resulted as an indirect effect of NBT-272.** Because NBT-272 was originally described as a MYC inhibitor, we evaluated the correlation of the expression of c-MYC and MYCN in the ET cell lines (Fig. 1S) with cell sensitivity to the compound. However, only the MB cell line D341 (bearing *c-MYC* amplification) was significantly more sensitive to NBT-272 than DAOY cells expressing *c-MYC* as single copy gene (Fig. 1) (16), whereas cells from other ET entities displayed a similar sensitivity to NBT-272 (Fig. 1).

Moreover, again regardless of the MYC isoform expressed and the gene copy number of *c-MYC/MYCN*, NBT-272 induced depletion of MYC in several ET cell lines, although exclusively at the protein level (Fig. 4A). In contrast, mRNA expression was either left almost unchanged (e.g. *MYCN* in SK-N-BE cells) or was enhanced (e.g. *c-MYC* in D341 cells) by NBT-272 in a dose-dependent manner (Fig. 4A).

The MYC family of transcription factors is known to have short half-lives (31). Therefore, we researched whether NBT-272 could have an effect on protein stability, thus helping to explain MYC depletion. In fact, by using the proteasome inhibitor MG132 (32) in

combination with NBT-272, c-MYC was already almost completely rescued after 4 h (Fig. 4B).

Additional lines of evidence supported an indirect effect of NBT-272 on MYC. Two small-molecule inhibitors specifically targeting the MYC/Max interaction (33, 34) did not show the same profile of activity as NBT-272 (Fig. 4C). In fact, significant cell viability could still be measured at high doses of both Mycro3 and 10058-F4. In particular, WAC-2 cells were almost unaffected by either of the compounds, whereas $10^3$-times less concentrated NBT-272 completely arrested cellular growth.

Finally, only a limited number of gene expression changes induced by NBT-272 matched with the transcriptional effects of siRNA-mediated silencing of *c-MYC* in DAOY cells (Fig. 6S, 4D). In fact, only a restricted number of genes were up-/downregulated in both sets of experiments, i.e. 11 apoptosis-related and 11 cell cycle-related transcripts (out of 84 in each analysis). Among them, even fewer genes were known direct targets of c-MYC (i.e. GADD45A, BIRC3, DFFA, CDK6, CDKN1A/p21, and PCNA). On the other hand, genes reported to be MYC targets exhibited a different expression profile, i.e. they were mostly downregulated in *c-MYC*-depleted cells, but induced or left unchanged in cells treated with NBT-272 (e.g. the cyclins CCNB1, CCNB2, CCND2, CCNH, and the DNA replication regulators MCM4 and MCM5).

Altogether, these results led us to conclude that a direct inhibition of MYC is unlikely to explain the effects triggered by NBT-272 in ET cells, which are more likely to be the result of more complex mechanisms and of interference with upstream pathways.

**NBT-272 targeted components of the AKT and ERK signaling pathways.** In order to improve our understanding of the regulatory mechanisms leading to arrest of the cell cycle, apoptosis, and autophagy, we analyzed the activation status of two signaling pathways, i.e. the

AKT/mTOR and the MEK/ERK pathways, regulating these cellular responses (35). Furthermore, both pathways have been documented to be relevant also in the development of ET.

Fig. 5A shows the effect of NBT-272 on the activation status of AKT varying in different cell lines, with phosphorylation at Ser473 significantly decreasing in WAC-2, SK-N-BE, and SH-SY5Y cell lines, but slightly enhanced in DAOY cells. On the other hand, the level of phosphorylated ERK 1/2 (p44/p42) diminished in all cell lines tested, although with different kinetics (Fig. 5A), suggesting a different sensitivity of the two pathways to NBT-272. In order to test whether NBT-272 had a direct effect on the enzymatic activity of either AKT or ERK and could thus be regarded as a kinase inhibitor, we quantified the *in vitro* kinase activity of 271 purified recombinant kinases (Fig. 7SA). However, none of them were significantly impaired by NBT-272 (20 nM). Additionally, different subunits and isoforms of phosphoinositide-3 kinase (PI3K) were tested (Fig. 7SB), again showing no effect from NBT-272 (20 nM).

Although the exact mechanism of action of NBT-272 remained unsolved, the compound clearly affected AKT- and ERK-dependent cellular functions. The downstream target of ERK, MNK1 (36), was also deactivated upon treatment with NBT-272, whereas the upstream kinase MEK1/2 was only slightly affected (Fig. 5A). MNK1 is known to phosphorylate both eIF4E and its repressor, 4EBP-1 (37). 4EBP-1 is also a direct target of mTOR, playing a key role as regulator of protein translation downstream of AKT (22). Interestingly, regardless of the AKT activation status, phosphorylation of both eIF4E and 4EBP-1 was impaired by NBT-272 in MB and NB cells (Fig. 5B), thus preventing the cap-dependent protein translation machinery from being completely functional. Additionally, the phosphorylation status of the ribosomal S6 protein, target of mTOR via S6 kinase (S6K) (38), was proven to be unaffected, thus reinforcing the idea of a 4EBP-1-dependent block of protein synthesis.

Moreover, we asked whether the cellular sensitivity to NBT-272-mediated G1/S block of the cell cycle, apoptosis, or autophagy would vary if one of the pathways had been affected by using specific inhibitors. To test the relevance of the mTOR/AKT pathway, BEZ235 was used (39). A pre-treatment with the PI3K/mTOR inhibitor increased both depletion of CCND1 and degradation of SQSTM1/p62 when compared to NBT-272 alone (Fig. 8SA), whereas no significant enhancement of the pro-apoptotic functions of NBT-272 was observed (Fig. 8SB). Although BEZ235 alone had apparently no effect, under these conditions, on the expression of the cell cycle and autophagy markers in DAOY cells, the inhibitor was functional, as demonstrated by the strong deactivation of AKT (Fig. 8SA) and the induction of apoptosis (Figure 8SB).

**NBT-272 blocked tumor progression in a xenograft model of NB.** NB cells bearing a transgene encoding luciferase (SH-SY5Y-LUC) were injected in the flank of ten athymic nude mice and were allowed to develop for three weeks. The effect of the i.p. administration of NBT-272 (10 μM/week) and of the vehicle (0.003% EtOH/PBS) on the tumor growth was monitored by quantifying the luminescent signal from engrafted SH-SY5Y-LUC cells. After six weeks of treatment, the tumors almost stopped growing in the mice receiving NBT-272, whereas the human NB SH-SY5Y cells expanded into large tumors in the control animals (6A, B and 9S). In fact, a 6.3-fold increase of tumor size could be detected in the control group compared with the NBT-272-treated ($p = 0.037$ according to Student's t-test). The result clearly indicated that NBT-272 has a significant anti-proliferative effect on the tumor development *in vivo*. The hemotoxylin/eosin staining of some representative tumor samples showed a compact and rounded shape of the tumors, which were characterized by a very dense cell distribution with some necrotic areas (Fig. 6C, panel a-d). Tumors from NBT-272-treated mice showed a clear reduction of Ki67-positive cells (Fig. 6C, panels f, h), whereas a

prominent cellular perinuclear staining in vehicle-treated mice was observed (panels e, g), thus confirming the significant anti-proliferative effect of NBT-272 also *in vivo*. Activation of caspase-3 was also evaluated (panels i, l) and show that the treatment with NBT-272 did not induce a significantly higher induction of apoptosis as compared to control tumors. This result confirmed our findings *in vitro* (Fig. 3A, B) by referring to the same cellular model, i.e. SH-SY5Y cells, which were used to induce the tumors. Finally, NBT-272 treatment had an effect on MYC stability/expression in the tumors, in which ERK activation was also impaired (Fig. 6D).

## Discussion

A fine regulation of protein turnover by a tunable modulation of protein stability requires specific post-translation modifications (such as phosphorylation) of key molecules. Many of these molecules are significant components of pro-survival pathways and often play a crucial role in tumor development and progression, in conditions of constitutive and growth factors-independent activation. In past decades, great efforts have been made to interfere with those signaling pathways by employing different strategies of targeted therapy, ranging from antibodies against receptor tyrosine kinases (RTK) to small-molecule inhibitors blocking downstream signaling effectors. Downstream of RTK activation, the induction of MYC transcription factors and of their pleiotropic effects on cell growth has been frequently associated with neoplastic transformation. Therefore, MYC itself clearly represents an attractive target for anti-cancer therapy (40), also due of its correlation with poor prognosis and high grade malignancy in many types of tumors, including pediatric malignancies (10, 11, 41, 42).

In the context of MYC-overexpressing ET tumors, we wanted to investigate the biological responses of a group of ET-derived cell lines to NBT-272, a small molecule of about 550 Da, previously described as inhibitor of MYC (15, 16). Its toxicity and ability to prevent colony formation *in vitro* indicated a very strong effect of NBT-272 at low concentrations.

In the search for an association between toxicity of NBT-272 and MYC expression levels in different ET cell lines, no significant correlation could be found. This observation led us to question any direct effect of NBT-272 on the oncogene, which would more likely be the result of different mechanisms, such as interference with protein synthesis and stability, affecting also the MYC family members known to have short half-lives (31). Indeed, we could observe

that inhibition of the proteasome-dependent protein degradation pathway restored the depleting effect of NBT-272 and almost completely stabilized c-MYC. Moreover, the effect induced by two specific MYC/Max inhibitors (33, 34) and by *c-MYC* silencing in ET cells did not match the cellular response to NBT-272, again detrimental to the hypothesis of a direct effect on MYC. This conclusion, however, certainly does not exclude that MYC inhibition contributed to the panel of cellular responses observed upon NBT-272 treatment.

Even though the compound is not a direct kinase inhibitor, our study indicated the ability of NBT-272 to interfere with the activation status of different components of the AKT/mTOR and MEK/ERK signaling pathways. We therefore attributed the effect of NBT-272 on apoptosis, cell cycle, and autophagy to its ability to interfere with these pathways. Indeed, the basal level phosphorylation of ERK1/2, MNK1, and AKT in MB and NB cells was impaired by NBT-272, under the same conditions that induced efficient cell cycle arrest (G1/S) and autophagosome formation. It is also relevant to emphasize that the two pathways converge to regulate the activation status of eIF4E and 4E-BP1, both dephosphorylated (i.e. inactive) in the presence of NBT-272, thus leading us to speculate that targeting these pathways would prevent full activation of the cap-dependent protein translation machinery. Furthermore, MYC depletion could possibly be explained, not only as an effect of protein synthesis inhibition, but also as a consequence of decreased phosphorylation at its Ser62 residue, which has a stabilizing effect and is catalyzed by ERK (43).

In total, our observations strongly suggest that both the AKT and MEK/ERK signaling pathways participate in orchestrating the cellular responses to NBT-272, at least *in vitro*. Moreover, combination of NBT-272 with a specific inhibitor of PI3K/mTOR, BEZ235 (39), seemed to further increase the NBT-272-dependent effect on cell cycle and autophagy, but not apoptosis. Numerous components of the AKT/mTOR and MEK/ERK pathways have been found deregulated in cancer, including ET. High basal activation levels of AKT and of the S6

ribosomal protein were documented in MB (44, 45) and a relevant role in NB pathogenesis was attributed to PI3K, found to be overexpressed in NB tumors (46). Phosphorylation of AKT, S6, and ERK has also been reported as a frequent event in NB, in which AKT activation in particular was correlated with diverse indicators of aggressive disease and poor prognosis (47). These two signaling pathways were also negatively associated with malignancy in childhood rhabdomyosarcoma (48) and in Ewing's sarcoma (49), thus rendering it certainly worthwhile to promote the idea of developing common therapeutic strategies effective in different ET entities.

Finally, NBT-272 arrested tumor growth in a xenograft model of human NB, showing that the potent effect of this compound could also be reproduced *in vivo*, with concomitant reduction of MYC expression and of ERK activation in the treated tumors. This very encouraging results warrant the extension of investigations to more ET models.

In summary, NBT-272 induced a relatively complex pattern of cellular responses, including inhibition of crucial regulators of protein synthesis. All these events could be related functionally to interference with key cell survival pathways (AKT and MEK/ERK) playing a role in the pathogenesis of several ETs. Our findings increase the present level of understanding of the mechanisms of action of NBT-272, explaining its potent anti-tumor effect in *in vitro* as well as *in vivo* models of ET. This study certainly justifies further efforts to define more clearly the potential benefits of using NBT-272 in novel therapeutic strategies for pediatric tumors.

## Acknowledgements

We acknowledge Dr. Brian Carter for his precious contribution in proofreading the manuscript and Dr. Beat Bornhauser and Prof. Shida Yousefi for helpful discussion. We are grateful to Lawrence Helson and James McChesney for providing NBT-272, developed by Tapestry Pharmaceuticals (Boulder, CO). We also thank Thererse Bruggmann and Gery Barmettler for their excellent technical support during the preparation and analysis of samples for electron microscopy.

## References

1. Scotting PJ, Walker DA, Perilongo G. Childhood solid tumours: a developmental disorder. Nat Rev Cancer 2005;5:481-8.

2. Grimmer MR, Weiss WA. Childhood tumors of the nervous system as disorders of normal development. Curr Opin Pediatr 2006;18:634-8.

3. Guessous F, Li Y, Abounader R. Signaling pathways in medulloblastoma. J Cell Physiol 2008;217:577-83.

4. Packer RJ. Childhood brain tumors: accomplishments and ongoing challenges. J Child Neurol 2008;23:1122-7.

5. Schwab M, Westermann F, Hero B, Berthold F. Neuroblastoma: biology and molecular and chromosomal pathology. Lancet Oncol 2003;4:472-80.

6. Maris JM. The biologic basis for neuroblastoma heterogeneity and risk stratification. Curr Opin Pediatr 2005;17:7-13.

7. Schwab M, Ellison J, Busch M, Rosenau W, Varmus HE, Bishop JM. Enhanced expression of the human gene N-myc consequent to amplification of DNA may contribute to malignant progression of neuroblastoma. Proc Natl Acad Sci U S A 1984;81:4940-4.

8. Bordow SB, Norris MD, Haber PS, Marshall GM, Haber M. Prognostic significance of MYCN oncogene expression in childhood neuroblastoma. Journal of Clinical Oncology 1998;16:3286-94.

9. Grotzer MA, Hogarty MD, Janss AJ, et al. MYC messenger RNA expression predicts survival outcome in childhood primitive neuroectodermal tumor/medulloblastoma. Clin Cancer Res 2001;7:2425-33.

10. Pomeroy SL, Tamayo P, Gaasenbeck M, et al. Prediction of central nervous system embryonal tumour outcome based on gene expression. Nature 2002;415:436-42.

11. Stearns D, Chaudhry A, Abel TW, Burger PC, Dang CV, Eberhart CG. c-myc overexpression causes anaplasia in medulloblastoma. Cancer Res 2006;66:673-81.

12. Schmidt EV. The role of c-myc in cellular growth control. Oncogene 1999;18:2988-96.

13. Rosati A, Quaranta E, Ammirante M, Turco MC, Leone A, De Feo V. Quassinoids can induce mitochondrial membrane depolarisation and caspase 3 activation in human cells. Cell Death Differ 2004;11 Suppl 2:S216-8.

14. Cuendet M, Pezzuto JM. Antitumor activity of bruceantin: an old drug with new promise. J Nat Prod 2004;67:269-72.

15. Helson L, McChesney, J., Bartyzel, P. In vitro cytotoxic activity of NBT-272, a novel quassinoid analog. 2004; Geneva: Eur J Cancer Suppl; 2004. p. 171.

16. von Bueren AO, Shalaby T, Rajtarova J, et al. Anti-proliferative activity of the quassinoid NBT-272 in childhood medulloblastoma cells. BMC Cancer 2007;7:19.

17. Fukamiya N, Lee KH, Muhammad I, et al. Structure-activity relationships of quassinoids for eukaryotic protein synthesis. Cancer Lett 2005;220:37-48.

18. Lachance PE, Miron M, Raught B, Sonenberg N, Lasko P. Phosphorylation of eukaryotic translation initiation factor 4E is critical for growth. Mol Cell Biol 2002;22:1656-63.

19. De Benedetti A, Harris AL. eIF4E expression in tumors: its possible role in progression of malignancies. Int J Biochem Cell Biol 1999;31:59-72.

20. Bjornsti MA, Houghton PJ. Lost in translation: dysregulation of cap-dependent translation and cancer. Cancer Cell 2004;5:519-23.

21. Pyronnet S. Phosphorylation of the cap-binding protein eIF4E by the MAPK-activated protein kinase MNK1. Biochem Pharmacol 2000;60:1237-43.

22. Sun SY, Rosenberg LM, Wang X, et al. Activation of AKT and eIF4E survival pathways by rapamycin-mediated mammalian target of rapamycin inhibition. Cancer Res 2005;65:7052-8.

23. Garcia de Veas R, Schweigerer L, Medina MA. Modulation of the proteolytic balance plasminogen activator/plasminogen activator inhibitor by enhanced N-myc oncogene expression or application of genistein. Eur J Cancer 1998;34:1736-40.

24. Garzia L, Andolfo I, Cusanelli E, et al. MicroRNA-199b-5p impairs cancer stem cells through negative regulation of HES1 in medulloblastoma. PLoS One 2009;4:e4998.

25. van den Heuvel S, Harlow E. Distinct roles for cyclin-dependent kinases in cell cycle control. Science 1993;262:2050-4.

26. Harbour JW, Luo RX, Dei Santi A, Postigo AA, Dean DC. Cdk phosphorylation triggers sequential intramolecular interactions that progressively block Rb functions as cells move through G1. Cell 1999;98:859-69.

27. Tasdemir E, Galluzzi L, Maiuri MC, et al. Methods for assessing autophagy and autophagic cell death. Methods Mol Biol 2008;445:29-76.

28. Faivre S, Kroemer G, Raymond E. Current development of mTOR inhibitors as anticancer agents. Nat Rev Drug Discov 2006;5:671-88.

29. Ohsumi Y, Mizushima N. Two ubiquitin-like conjugation systems essential for autophagy. Semin Cell Dev Biol 2004;15:231-6.

30. Pankiv S, Clausen TH, Lamark T, et al. p62/SQSTM1 binds directly to Atg8/LC3 to facilitate degradation of ubiquitinated protein aggregates by autophagy. J Biol Chem 2007;282:24131-45.

31. Sears RC. The life cycle of C-myc: from synthesis to degradation. Cell Cycle 2004;3:1133-7.

32. Kim D, Kim SH, Li GC. Proteasome inhibitors MG132 and lactacystin hyperphosphorylate HSF1 and induce hsp70 and hsp27 expression. Biochem Biophys Res Commun 1999;254:264-8.

33. Kiessling A, Wiesinger R, Sperl B, Berg T. Selective inhibition of c-Myc/Max dimerization by a pyrazolo[1,5-a]pyrimidine. ChemMedChem 2007;2:627-30.

34. Wang H, Hammoudeh DI, Follis AV, et al. Improved low molecular weight Myc-Max inhibitors. Mol Cancer Ther 2007;6:2399-408.

35. Song G, Ouyang G, Bao S. The activation of AKT/PKB signaling pathway and cell survival. J Cell Mol Med 2005;9:59-71.

36. O'Loghlen A, Gonzalez VM, Jurado T, Salinas M, Martin ME. Characterization of the activity of human MAP kinase-interacting kinase MNK1b. Biochim Biophys Acta 2007;1773:1416-27.

37. Richter JD, Sonenberg N. Regulation of cap-dependent translation by eIF4E inhibitory proteins. Nature 2005;433:477-80.

38. Ali SM, Sabatini DM. Structure of S6 kinase 1 determines whether raptor-mTOR or rictor-mTOR phosphorylates its hydrophobic motif site. J Biol Chem 2005;280:19445-8.

39. Maira SM, Stauffer F, Brueggen J, et al. Identification and characterization of NVP-BEZ235, a new orally available dual phosphatidylinositol 3-kinase/mammalian target of rapamycin inhibitor with potent in vivo antitumor activity. Mol Cancer Ther 2008;7:1851-63.

40. Grotzer MA, Castelletti D, Fiaschetti G, Shalaby T, Arcaro A. Targeting Myc in pediatric malignancies of the central and peripheral nervous system. Curr Cancer Drug Targets 2009;9:176-88.

41. Rouah E, Wilson DR, Armstrong DL, Darlington GJ. N-myc amplification and neuronal differentiation in human primitive neuroectodermal tumors of the central nervous system. Cancer Res 1989;49:1797-801.

42. Gilbertson RJ, Wickramasinghe C, Hernan R, et al. Clinical and molecular stratification of disease risk in medulloblastoma. British Journal of Cancer 2001;85:705-12.

43. Lutterbach B, Hann SR. Hierarchical phosphorylation at N-terminal transformation-sensitive sites in c-Myc protein is regulated by mitogens and in mitosis. Mol Cell Biol 1994;14:5510-22.

44. Guerreiro AS, Fattet S, Fischer B, et al. Targeting the PI3K p110alpha isoform inhibits medulloblastoma proliferation, chemoresistance, and migration. Clin Cancer Res 2008;14:6761-9.

45. Hartmann W, Digon-Sontgerath B, Koch A, et al. Phosphatidylinositol 3'-kinase/AKT signaling is activated in medulloblastoma cell proliferation and is associated with reduced expression of PTEN. Clin Cancer Res 2006;12:3019-27.

46. Boller D, Schramm A, Doepfner KT, et al. Targeting the phosphoinositide 3-kinase isoform p110delta impairs growth and survival in neuroblastoma cells. Clin Cancer Res 2008;14:1172-81.

47. Opel D, Poremba C, Simon T, Debatin KM, Fulda S. Activation of AKT predicts poor outcome in neuroblastoma. Cancer Res 2007;67:735-45.

48. Petricoin EF, 3rd, Espina V, Araujo RP, et al. Phosphoprotein pathway mapping: AKT/mammalian target of rapamycin activation is negatively associated with childhood rhabdomyosarcoma survival. Cancer Res 2007;67:3431-40.

49. Benini S, Manara MC, Cerisano V, et al. Contribution of MEK/MAPK and PI3-K signaling pathway to the malignant behavior of Ewing's sarcoma cells: therapeutic prospects. Int J Cancer 2004;108:358-66.

## Figure legends

**Figure 1. Dose-dependent effect of NBT-272 on cell viability and colony formation in ET-derived cell lines.** (A) Chemical structure of NBT-272. (B) MTS assays were performed 72 h after addition of increasing concentrations of NBT-272 (1-182 nM) in 13 ET-derived cell lines. (C) The $IC_{50}$ values relative to NBT-272 toxicity are listed, as calculated from the curves fitting the data in panel B. DAOY M2 cells (overexpressing c-MYC) are also reported. (D) Five cell lines were evaluated for anchorage-independent growth in soft agar. NBT-272 reduced colony formation by 50% relative to monolayer cultures at concentrations lower than/similar to $IC_{50}$ values. $IC_{50}$ (nM): WAC-2, 2.3; SK-N-BE, 4.3; A673, 4.6; MON, < 1; Wit-49, 9.7.

**Figure 2. Induction of cell cycle arrest in MB and NB cells**. (A) WAC-2, SK-N-BE, and SH-SY5Y cells were treated with the indicated amount of NBT-272 for 16 h, or were left untreated (control). The percentage of cells in different stages of the cell cycle is reported in each diagram. (B) WAC-2 and DAOY cells were subjected to treatment with 20 nM NBT-272 and analyzed for expression of cell cycle-regulatory proteins by immunoblotting at different time points. The experiment was also confirmed in SH-SY5Y cells treated for 16 h.

**Figure 3. NBT-272-induced apoptosis and autophagy in ET cell lines.** (A) Induction of apoptosis was quantified by Caspase-Glo 3/7 assay (Promega) in 10 cell lines representative of different ET entities, following treatment with 10/20 nM NBT-272 for 24 h. Luminescence signals were normalized to cell viability (MTS assay). (B) Cleavage of PARP/caspase 3 was evaluated by western blotting in the MB cell lines D341 and DAOY and in two NB cell lines (SH-SY5Y and SK-N-BE), treated as indicated. The apparent molecular weight of full length

and cleaved caspases-3 on the blots is indicated (35 kDa, 17-19 kDa) (C) High resolution electron microscopy was performed to analyze the effect of NBT-272 (20 nM, 16 h) on the ultrastructural organization of DAOY cells (a, c-e, h) and of SK-N-BE cells (b, f, g). Mock-treated cells (a, b) appeared healthy with homogeneous cytoplasm and regular nuclear envelope. Treated cells displayed a looser cytosol and membrane blebbing at the cell surface (c) as well as a drastic increase in the amount of vacuoles and lysosomes (c, d). Numerous autophagosomes containing cellular fragments, ribosomes, and whole mitochondria could be detected (arrow heads). DAOY cells were treated separately with rapamycin (200 nM, 48 h) as control (h). Bars: a, h = 4µm, b-d, g = 2 µm, e, f = 0.5 µm. (D) Change in expression of the autophagy-related proteins SQSTM1 (p62) and LC-3 and of the Atg5-12 complex (markers of autophagosome formation) was documented by immunoblotting in DAOY cells.

**Figure 4. Indirect effect of NBT-272 on MYC.** (A) The effect of NBT-272 on either c-MYC or MYCN in different ET cell lines was analyzed at the protein (western blotting) and at the mRNA level (qRT-PCR). (B) Cotreatment of D341 cells with MG132, inhibiting proteasome-mediated protein degradation, rescued c-MYC from the depleting effect of NBT-272. (C) Cell viability was evaluated in three NB-derived cell lines (SK-N-BE, SH-SY5Y, WAC-2) incubated for 72 h with increasing doses of Mycro3 (33) or 10058-F4 (34). (D) Changes in the expression of apoptosis- (left) and cell cycle-related genes (right) were analyzed comparing the effect of NBT-272 (1) and of *c-MYC* down-regulation by siRNA (2). For the silencing experiment, DAOY M2 cells were transfected transiently with *c-MYC* siRNA and gene expression was analyzed after 48 h by using the RT² Profiler™ PCR Array. The same cell line was treated for 24 h with 20 nM NBT-272 and subjected to the same analysis. Results in the hit maps are expressed as the log2Ratio (Ratio=2^-ΔΔCt), obtained from NBT-272-treated or *c-MYC* siRNA-transfected cells normalized to the corresponding controls (i.e.

mock-treated and control siRNA-transfected cells, respectively). Values in each analysis represent the average of three independent experiments.

**Figure 5. Inhibition of protein translation and of the AKT/mTOR- and ERK-dependent pathways**. (A) Protein expression and activation status of components of the AKT/mTOR and ERK pathways were investigated by immunoblotting. (B) Treatment with NBT-272 triggered a depletion of active eIF4E and 4EBP-1 proteins in different cell lines as early as 16 h.

**Figure 6. Reduction of tumor growth induced by NBT-272 in a xenograft model.** Female athymic nude mice were injected in the right flank with SH-SY5Y-LUC cells. Three weeks after injection, the mice were divided into two homogeneous groups (based on the amount of engrafted human cells). The mice received either NBT-272 (10 μM/week) or vehicle (0.003% EtOH/PBS), both administered three times a week. (A) The tumor growth rate was monitored on a weekly basis by quantifying the luciferase activity of the recombinant tumor cells *in vivo* (see scale bars) and plotted starting from the first day of treatment. Blue: vehicle-treated animals. Red: NBT-272-treated animals. BLI data are available as a supplementary figure (Fig. 7S). (B) Quantification of the tumor growth rate. (C) H&E and IHC staining of tumor samples obtained from mice treated either with vehicle alone (left panels) or with NBT-272 (right panels), according to the described protocol. The panels c-d represent the enlarged view of the selected areas in panels a-b, respectively. In a-b the tumors are shown as hyper-dense rounded structures with some necrosis portions (n). In panels e-g, the tumor sections were stained for Ki67 (proliferation), whereas in panels i-l the staining for cleaved caspase-3 (cl-CASP3, apoptosis) is shown. Images a-b: 5x magnification, images c-l: 40x magnification.

(D) Western blotting detection of c-MYC, p-ERK1/2, and p-AKT was performed in total protein extracts from tumors developed by mice 4 (vehicle-treated) and 9 (NBT-272-treated).

# Figure 1

A

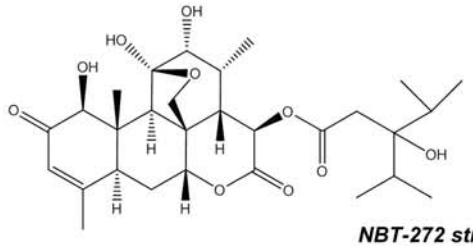

*NBT-272 structure*

B

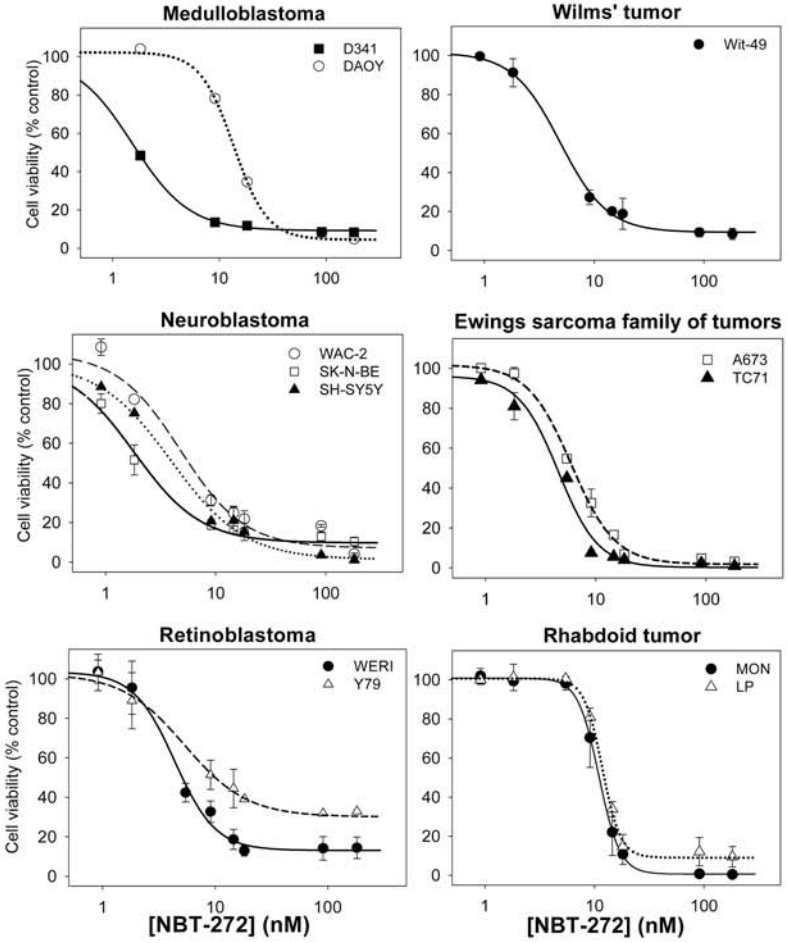


C

| ET entity | Abbr. | Cell line | [NBT-272] $IC_{50}$ (nM) |
|---|---|---|---|
| Medulloblastoma | MB | DAOY | 13.6 |
| | | DAOY M2 | 4.9 |
| | | D341 | 1.5 |
| Neuroblastoma | NB | WAC-2 | 4.8 |
| | | SK-N-BE | 1.8 |
| | | SH-SY5Y | 3.5 |
| Retinoblastoma | RB | WERI | 4.4 |
| | | Y79 | 5.4 |
| Wilms' tumor | WT | Wit-49 | 4.9 |
| Ewing sarcoma family of tumors | ESFT | A673 | 6.0 |
| | | TC71 | 4.6 |
| Malignant rhabdoid tumor | MRT | MON | 11.8 |
| | | LP | 11.0 |

D

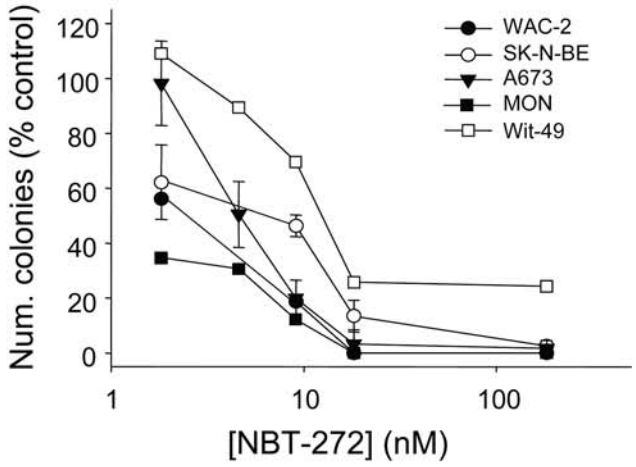

**Figure 2**

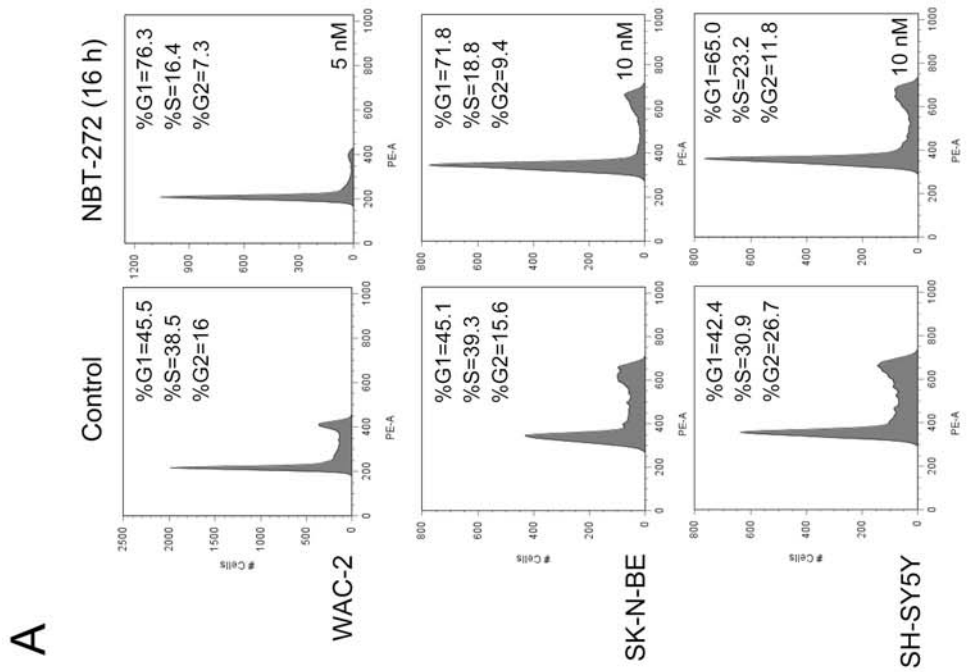


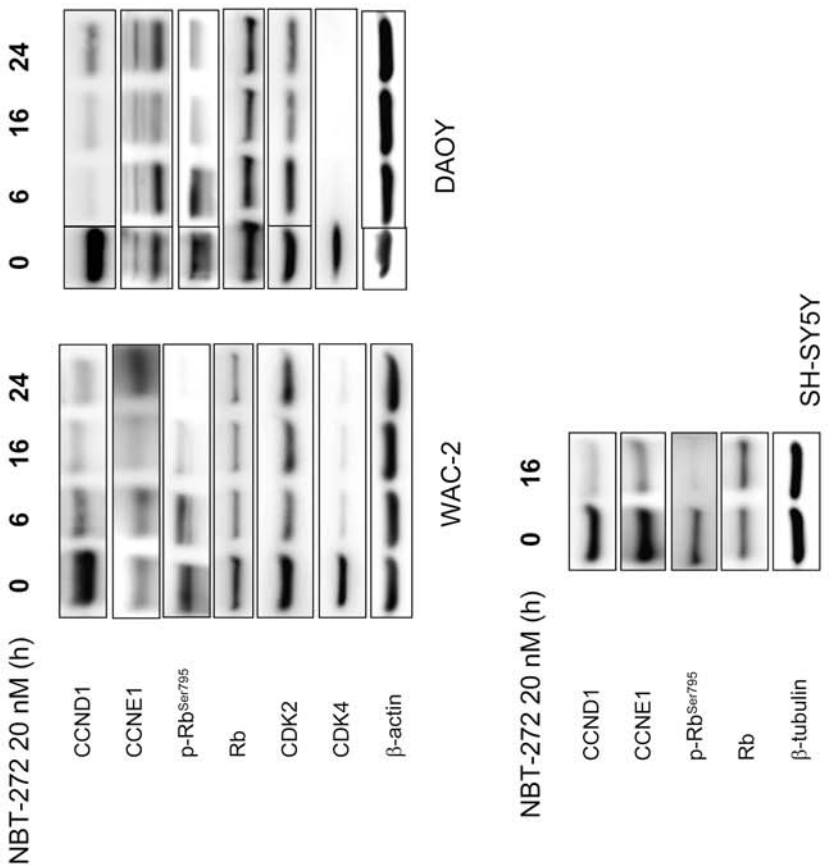

Author Manuscript Published OnlineFirst on October 1, 2010; DOI: 10.1158/1535-7163.MCT-10-0539
Author manuscripts have been peer reviewed and accepted for publication but have not yet been edited.

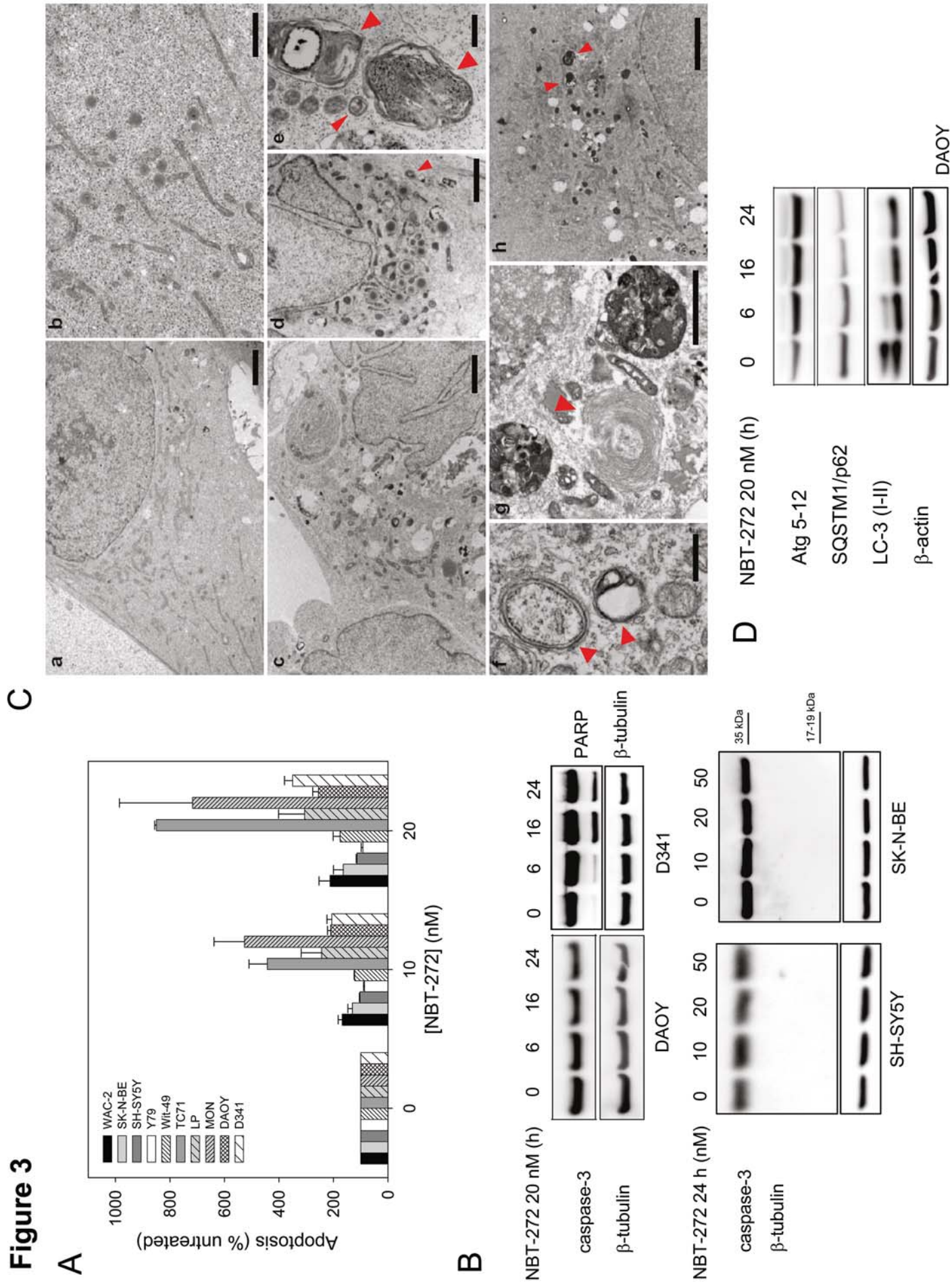

**Figure 4**

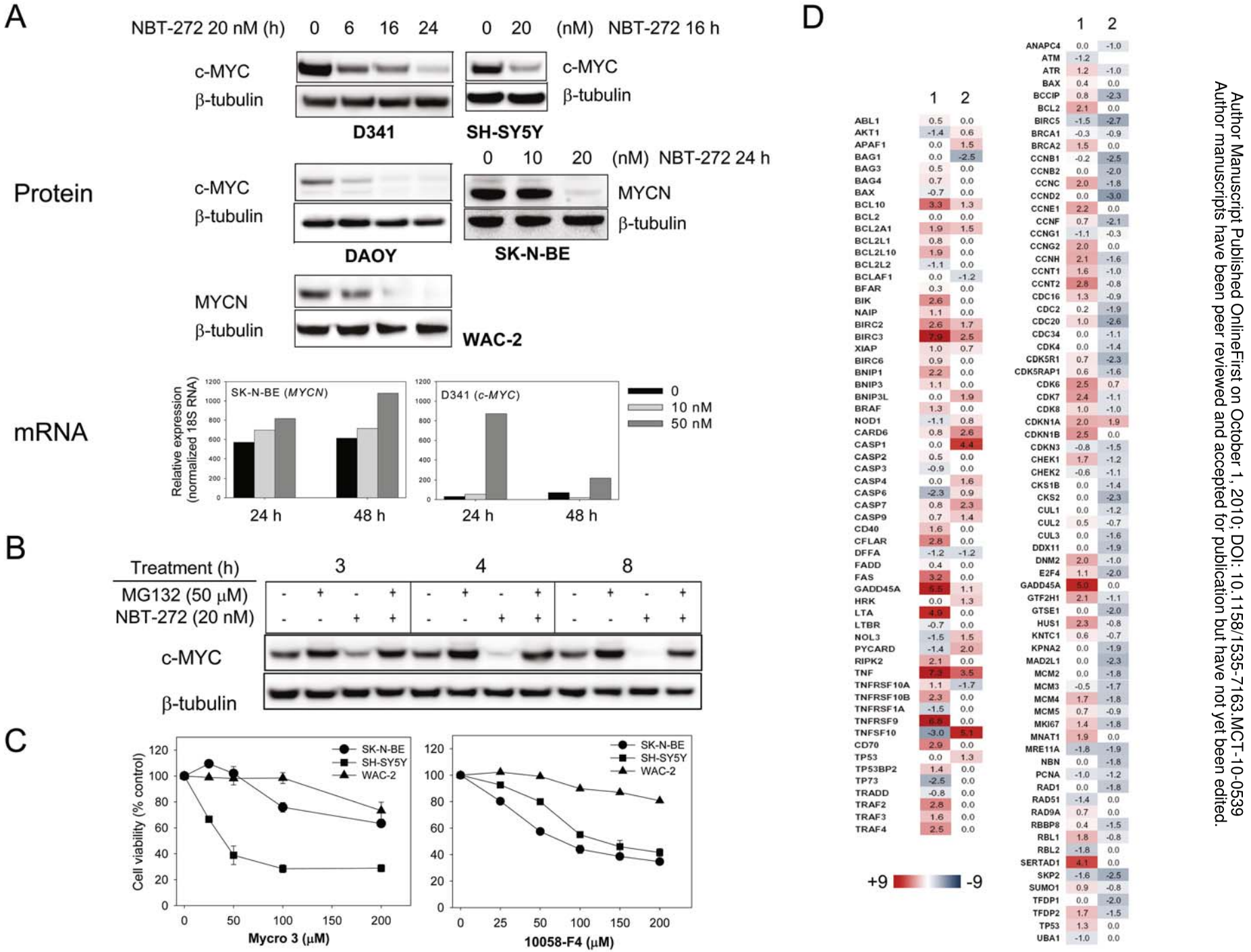

**Figure 5**